Synthetic virus-like particles and conformationally constrained peptidomimetics in vaccine design

Riedel, T ; Ghasparian, A ; Moehle, K ; Rusert, P ; Trkola, A ; Robinson, J A

Abstract: Conformationally constrained peptidomimetics could be of great value in the design of vaccines targeting protective epitopes on viral and bacterial pathogens. But the poor immunogenicity of small synthetic molecules represents a serious obstacle for their use in vaccine development. Here, we show how a constrained epitope mimetic can be rendered highly immunogenic through multivalent display on the surface of synthetic virus-like nanoparticles. The target epitope is the V3 loop from the gp120 glycoprotein of HIV-1 bound to the neutralizing antibody F425-B4e8. The antibody-bound V3 loop adopts a -hairpin conformation, which is effectively stabilized by transplantation onto a D-Pro-L-Pro template. The resulting mimetic after coupling to synthetic virus-like particles elicited antibodies in rabbits that recognized recombinant gp120. The elicited antibodies also blocked infection by the neutralization sensitive tier-1 strain MN of HIV-1, as well as engineered viruses with the V1V2 loop deleted; this result is consistent with screening of V3 by the V1V2 loop in intact trimeric viral gp120 spikes. The results provide new insights into HIV-1 vaccine design based on the V3 loop, and illustrate how knowledge from structural biology can be exploited for the design of constrained epitope mimetics, which can be delivered to the immune system by using a highly immunogenic synthetic nanoparticle delivery system.

DOI: https://doi.org/10.1002/cbic.201100586

Synthetic Virus-Like Particles and Conformationally Constrained Peptidomimetics in Vaccine Design

Tina Riedel[1], Arin Ghasparian[1], Kerstin Moehle[1], Peter Rusert[2], Alexandra Trkola[2] and John A. Robinson[1]*

[1] Chemistry Department, and [2] Institute of Medical Virology,

University of Zurich, Winterthurerstrasse 190, 8057 Zurich, Switzerland.

Correspondence to:

Prof. John A. Robinson,

Chemistry Department

University of Zurich

Winterthurerstrasse 190

8057 Zurich

Switzerland

Tel: +41-44-6354242

Fax: +41-44-6356812

E-mail: robinson@oci.uzh.ch

Abstract:

Conformationally constrained peptidomimetics may be of great value in the design of vaccines targeting protective epitopes on viral and bacterial pathogens. But the poor immunogenicity of small synthetic molecules represents a serious obstacle for their use in vaccine development. Here, we show how a constrained epitope mimetic can be rendered highly immunogenic through multi-valent display on the surface of synthetic virus-like nanoparticles. The target epitope is the V3 loop from the gp120 glycoprotein of HIV-1 bound to the neutralizing antibody F425-B4e8. The antibody-bound V3 loop adopts a ß-hairpin conformation, which is effectively stabilized by transplanting onto a D-Pro-L-Pro template. The resulting mimetic after coupling to synthetic virus-like particles elicited antibodies in rabbits that recognized recombinant gp120. The elicited antibodies also blocked infection by the neutralization sensitive tier-1 strain MN of HIV-1, as well as engineered viruses with the V1V2 loop deleted, a result consistent with screening of V3 by the V1V2 loop in intact trimeric viral gp120 spikes. The results provide new insights into HIV-1 vaccine design based on the V3 loop, and illustrate how knowledge from structural biology can be exploited for the design of constrained epitope mimetics, which can be delivered to the immune system using a highly immunogenic synthetic nanoparticle delivery system.

Introduction

Preventive vaccine design has traditionally been approached empirically through immunizations with dead or attenuated microorganisms to induce protective immunity.[1] Considering the complexity of such vaccine preparations, it is not suprising that little is understood at a molecular level about their pharmacology and detailed mechanism(s) of action in the host.[2] More recently, the focus in vaccine design has shifted to subunit vaccines, where protein subunits are used to generate a protective immune response. Reverse vaccinology approaches can exploit advances in microbial genomics and proteomics to enable high-throughput production and testing of recombinant microbial proteins, in order to identify potential protein-based vaccine candidates.[3] Difficulties arise, however, because recombinant proteins tend to be poorly immunogenic, and so they are typically administered together with immunostimulatory adjuvants.[4] Moreover, the reactogenicity of some of the most potent preclinical adjuvants and the cost and complexity of licensing new adjuvants for human use remains a serious problem.[4, 5] Recombinant proteins may also be incorrectly folded, and may expose irrelevant epitopes that are normally hidden on the pathogen surface, leading generally to poorly protective immune responses. The use of peptides to focus immune responses on protective surface epitopes has also attracted great interest.[6] However, linear peptides are flexible and so often do not mimic well conformational protein epitopes, they tend to have an unfavorable pharmacology *in-vivo* due to proteolysis, and their ability to induce humoral immune responses (immunogenicity) is again very poor. These factors may explain why no peptide-based vaccine has so far been developed for human use.

Most preventive vaccines are based on the induction of neutralizing antibodies in the host, which recognize protective epitopes on the surfaces of bacteria or viruses. The mechanisms by which the immune system is activated are now becoming increasingly well understood at the molecular and cellular levels. Important signals for the activation of

immune cells are provided by; 1) repetitive multi-valent display of B-cell epitopes across a bacterial or viral surface, to cross-link cell-surface B-cell receptors and stimulate B-cell activation[7, 8]; 2) peptide fragments comprising T-cell epitopes derived from pathogen proteins produced inside antigen presenting cells (e.g. dendritic cells), are displayed in complexes with MHC-I and -II proteins on the cell surface, where they are recognized by T-cell receptors on T-cells.[9] Activated T-cells then provide crucial help to B-cells during the maturation phase of the adaptive immune response; 3) dendritic cells (DCs) are the sentinel cells in the body that can sense invading microorganisms and alert other cells of the immune system.[10] Their cell surface receptors allow efficient uptake and internalization of soluble or particulate matter in the periphery, leading to proteolytic processing of internalized protein antigens and MHC presentation of peptide fragments. After migration to and entry into the lymph nodes, surface bound antigens on dendritic cells are screened by B-cells,[11] whereas peptide-MHC complexes on the cell surface are screened by T-cells. In addition, already in the periphal tissues DCs become activated, by sensing microbial products using innate immunity receptors such as those belonging to the Toll-like Receptor (TLR) family.[12, 13] This leads to up-regulation of MHC expression, production of immunostimulatory cytokines, and enhanced migration to the lymph nodes. Knowledge of these mechanisms of immune activation at a molecular level opens new possibilities for vaccine design, using rational structure-based methods.

In earlier work, we reported the design of synthetic lipopeptide conjugates that have the ability to spontaneously self-assemble in aqueous solution into small and remarkably homogeneous virus-sized nanoparticles of ca. 20-30 nm diameter, called synthetic virus-like particles (SVLPs).[14-16] The design of the lipopeptides is guided by knowledge that some lipopeptides of bacterial origin containing Pam_2Cys or Pam_3Cys, are TLR ligands.[17, 18] T-cell epitopes can also be incorporated into the peptide portion of the lipopeptide, and B-cell

epitopes can be added such that after SVLP formation, multiple copies of the epitope are displayed over the particle surface. Hence, some of the key immunostimulatory signals required for immune activation are present in a nanoparticle, which can be produced from a synthetically-derived molecule. We have shown that SVLPs can be used to elicit strong humoral immune responses in animal models without the use of adjuvants, including in one example, antibodies that could recognize a natural epitope on the malaria parasite.[16] We are interested to explore whether this delivery system can be further developed for vaccine use. Here we describe efforts to display conformationally constrained peptidomimetics on the surface of SVLPs, which offers the prospect of using knowledge from structural biology for epitope mimetic design. As a target antigen we chose the V3 loop in the gp120 envelope glycoprotein from HIV-1. We describe a highly effective method for producing accurate constrained mimics of this epitope, and show that the mimics can be used to elicit antibodies that neutralize infection by some strains of HIV-1.

HIV-1 entry into cells begins with binding of viral surface envelope glycoprotein trimers composed of non-covalently linked gp41 and gp120 subunits, to the cellular receptor CD4 on host cells.[19] This interaction triggers conformational changes within gp120 that increase exposure of the third variable region (V3) loop and a region of gp120 between the inner and outer domains that interacts with the co-receptor, either CCR5 or CXCR4.[20] This allows V3 to dock with the co-receptor extracellular surface, thereby stabilizing the complex.[21, 22]

The V3 region is typically a 35 amino acid, hypervariable, glycosylated and disulfide-bonded hairpin loop, with a highly conserved motif (GPGR/Q; residues 312-315 in the HXB2 numbering scheme[23]) in a ß-turn at the tip (Figure-1). A crystal structure of an engineered gp120 from strain JR-FL bound to CD4 and a neutralizing antibody (X5) Fab fragment (PDB 2B4C) revealed for the first time the intact V3 loop in an extended ß-hairpin conformation.[24]

Another crystal structure of an engineered gp120-CD4 complex bound to a tyrosine-sulfated antibody Fab (412d) (PDB 2QAD) revealed a more rigid V3 loop in a different ß-hairpin conformation, with the incoming and outgoing strands of the V3 stem closer together and the ß-hairpin structure again capped by a ß-turn (Figure-1).[21] In addition, a large number of crystal structures are available of various V3 loop-derived peptides bound to different neutralizing antibody Fab fragments, which reveal the V3 peptide in various ß-hairpin conformations.[25-29]

For this work, we started from a crystal structure of a V3 loop-derived peptide (sequence shown in Figure-1) bound to the human mAb F425-B4e8 (see Figure-2).[30] This antibody is able to neutralize cellular infection by a number of different HIV-1 strains, and so is an interesting target for the design of a vaccine able to elicit F425-B4e8-like antibodies.[31]

Results

Design of V3 loop mimetics

The crystal structure of a V3 loop-derived linear peptide bound to the antibody F425-B4e8 is shown in Figure-2. The V3 loop adopts a ß-hairpin conformation, with cross-strand residue pairs I307/Y318, and K305/T320 at hydrogen-bonding (HB) positions. The dipeptide D-Pro-L-Pro can be used as a template to stabilize hairpin conformations and to fix the hairpin register in macrocyclic hairpin mimetics.[32] The pair of residues directly attached to the template should orient their side chains onto the same face of the hairpin, and occupy a HB position adjacent to the template. In the ß-hairpin mimetic shown in Figure-2, the HB pair K305/T320 are directly attached to the template. The mimetic was synthesized by standard methods and purified by HPLC (see Supporting Information).[33]

Conformational studies

The structure of the mimetic in aqueous solution (H_2O/D_2O, pH 5.0) was investigated by NMR spectroscopy. Major and minor conformers were detected in solution that interconvert slowly, due to *cis-trans* isomerization (1:3 ratio) at the Gly-Pro peptide bond at the tip of the hairpin. Structural studies were pursued with the *trans*-form, which is present in excess (see Figure-3).

The $^3J_{HN\alpha}$ values were mostly >8Hz for residues expected to lie in ß-strands, consistent with the proposed ß-hairpin conformations.[34] All amide NH protons exchanged rapidly with solvent (within the time taken to measure a spectrum), and so were not helpful for identifying cross-strand hydrogen-bonded amide groups. However, the $\Delta\delta_{NH}/\Delta T$ temperature coefficients of residues predicted to occupy HB positions in ß-strands are lower (more positive than -4.5 ppb/K) than those for residues in NHB positions. In proteins, a temperature coefficient more positive than -4.5 ppb/k indicates a likely hydrogen bonded NH.[35, 36] Assuming here that no major changes occur in secondary structure in the constrained mimetics in the temperature range studied (all shift vs. temperature plots were linear), the $\Delta\delta_{NH}/\Delta T$ data support the hydrogen-bonded hairpin registers predicted in the design process.

^1H and ^{13}C chemical shift deviations from random coil values ($\Delta\delta=\delta^{observed} - \delta^{random}$) were examined to provide further evidence for regular secondary structure (see Supporting Information). Positive values for $\Delta\delta_{H\alpha}$ and $\Delta\delta_{C\beta}$ are expected for strands in ß-hairpins and negative values for $\Delta\delta_{C\alpha}$.[37-40] For the $\Delta\delta_{H\alpha}$ values, these expectations were largely observed (See Supporting Information), although the values are larger for the C-terminal strand than for the N-terminal strand of the ß-hairpin. The $\Delta\delta_{C\alpha}$ values were mostly in the negative

range, and the $\Delta\delta_{C\beta}$ values were mostly positive, as expected, for the strand regions of a ß-hairpin.

The strongest evidence for ß-hairpin conformations comes from analyses of NOEs. Key long-range NOEs detected in NOESY plots are shown in Figure-3. Notable is the extensive network of long range NOEs, between backbone protons (CαH and NH) in cross-strand residues at HB and NHB positions, as well as between the side chains of residues located on the same face of the hairpin, including backbone Hα-Hα NOEs between R306-T319 and H308-F317, HN-HN NOEs between K305-T320, and HN-Hα NOEs between I307-T319 and I309-F317. In addition, long range NOEs are seen between R306-F317, I307-Y318, Y309-Y318, F317-T319 and Y318 and T320.

In summary, the NMR data provide strong support for a stable ß-hairpin conformation in the mimetic. Average solution structures were calculated using NOE-derived distance constraints (results are shown in Table-1). The solution NMR structures all possess a ß-hairpin, and superimpose with a backbone rmsd of 1.01 Å. The tip region appears to be more flexible, adopting both type-I and type-II ß-turns (Figure-4). A comparison between the NMR structures for the mimetic and the antibody-bound V3 loop-derived peptide in crystal structure 2QSC, reveal excellent conformational mimicry of the antibody-bound peptide conformation (Figure-4).

Antigenicity studies

We found no published data on the affinity of the linear V3 peptide (called RP142) for the mAb F425-B4e8.[27, 31] However, a small amount of the F425-B4e8 antibody was available through the NIH AIDS Research and Reference Reagent Program, which was sufficient here for competition ELISA-based affinity comparisons.

For competition ELISA, biotinylated-RP142 was immobilized on microtitre plates coated with streptavidin (see Supporting Information). Plates were incubated with a fixed concentration of mAb F425-B4e8 and increasing concentrations of competing peptide (RP142 or ß-hairpin mimetic). In this way, IC_{50} values were determined for the competing linear peptide (IC_{50} = 3.4 nM) and the ß-hairpin mimetic (IC_{50} = 0.8 nM). The results show that the mimetic binds to the mAb with high affinity.

Immunogenicity studies

We asked whether the mimetic can elicit a humoral immune response that cross-reacts with gp120 and with envelope spikes on native virions. The mimetic was coupled to a lipopeptide carrier (**3**)[16] that can self-assemble into SVLPs (Figure-5).[14, 15] To conjugate the mimetic to the lipopeptide carrier, a hydrazine group was added to the L-Pro residue of the template, as shown by peptide **1** in Figure-5. After synthesis of the new cyclic mimetic (**1**), the hydrazino group could be reacted selectively with 4-maleimidobutyryl-*N*-hydroxysuccinimide ester to give **2**. The maleimido-labelled mimetic (**2**) was then coupled in high yield to the Cys residue in lipopeptide **3**,[16] to give **4** (Figure-5) (see Supporting Information). When dissolved in phosphate-buffered saline (PBS), this lipopeptide (**4**) assembles spontaneously into SVLPs with a mean hydrodynamic radius by dynamic light scattering of ca. 20-25 nm (see Supporting Information). Based on earlier precedence, about 60-80 copies of the mimetic should be displayed over the surface of each nanoparticle, as illustrated in Figure-5B.[15, 16]

SVLPs obtained from lipopeptide **4** were used to immunize three New Zealand white rabbits, each three times. Sera were collected after each immunization. After the third immunization, IgG end-point titres against the lipopeptide **4** were shown by ELISA to be in the range 20-30'000. Serum from the highest responding rabbit showed an end-point titre of

23'000 also against the mimetic (**1**) coupled to biotin (see Experimental section), and this anti-serum was used for for further study.

The ability of the elicited polyclonal IgG to bind to recombinant gp120 was assayed by ELISA and by surface plasmon resonance (SPR, BIAcore) biosensor. First, the IgG fraction in serum from the highest responding rabbit was isolated by protein-G affinity chromatography. IgG binding to recombinant gp120 was then detected by ELISA, and the binding could be competed away in the presence of mimetic (Figure-6A). Binding studies were also performed by immobilizing recombinant gp120 from either strain JR-FL or from strain LAI, on a CM5 sensor chip by random amine coupling. The LAI strain was used as a control, since the anti-mimetic antibodies are not expected to bind to gp120 from this strain, since the V3 loop in this strain has a two-residue (QR) insertion at the tip of the loop as well as several mutations in the flanking ß-strands (see Figure-1). As expected, the sensorgrams revealed a strong interaction between the anti-mimetic IgG and immobilized $gp120_{JR\text{-}FL}$, but not $gp120_{LAI}$ (see Supporting information). We conclude, therefore, that antibodies raised against the mimetic are able to recognize and bind recombinant gp120.

The neutralizing activity of the affinity-purified anti-mimetic IgG was tested using a luciferase reporter gene assay in TZM-bl cells, based upon single round infection with molecularly cloned Env-pseudotyped viruses.[41] The assays were performed with viruses pseudotyped with the envelopes of the neutralization sensitive, HIV-1 tier-1 strains MN and SF-162, and more neutralization resistant tier-2 viruses REJO and JR-FL, and the tier-3 virus 10.14. In addition, mutant envelopes of these viruses with deleted V1V2 loop regions were probed.[42] As shown in Figure-6B, only infection by the neutralization-sensitive laboratory MN strain was successfully inhibited by the anti-mimetic antibodies. None of the neutralization-insensitive strains isolated from HIV-infected humans were inhibited, unless the V1V2 loop region was first deleted. All the V1V2 mutant viruses, except REJO were

highly sensitive to neutralization by the anti-mimetic antibodies. The neutralizing activity could also be competed-out by adding excess mimetic, consistent with neutralization being dependent upon anti-mimetic IgG (Figure-6C). As controls, no effects were observed upon infection by murine leukaemia virus envelope pseudotyped virus, and no inhibitory activity was seen for the pre-immune IgG fraction from the rabbits (not shown).

Discussion

Structural vaccinology is an emerging technology in vaccine development.[43] An increasing number of publications document the value of structural biology in defining the 3D structures of epitopes recognized by neutralizing antibodies on various pathogenic organisms. One way to exploit this structural information is to design synthetic peptidomimetics with defined conformations that can be used to elicit immune responses. However, a method is also needed to effectively target the mimetics to immune cells and elicit potent immune responses. In this work, we demonstrate one very effective method for generating mimetics of ß-hairpin epitopes, which can be rendered immunogenic by presentation on the surface of SVLPs.

The V3 loop of HIV-1 has been the focus of many earlier studies in vaccine design. Early structural studies focused on Fab fragments of mAbs generated against conformationally flexible linear and disulfide-bridged V3-derived peptides.[44-50] Early efforts to constrain such V3-derived peptides included the replacement of the Ala in the loop tip (Figure-1) by the α-aminoisobutyryl (Aib) residue,[51] and backbone macrocyclization using a hydrazone link as a mimic of a cross-strand hydrogen bond.[46, 52, 53] Macrocyclic V3 loop mimetics have also synthesized, coupled to outer membrane proteins of *Neisseria meningitidis* and used for immunizations.[54, 55]

More recently structures of several V3-derived peptides bound to the murine anti-gp120 (HIV-1_{IIIB} strain) mAb (called 0.5ß) and to the human mAb 447-52D, were determined

by NMR.[56-59] An HIV-1_{IIIB}-derived peptide in complex with the 0.5ß mAb was shown to adopt a type-VI ß-turn at RGPG, with the central GP peptide bond in a *cis* conformation at the ß-hairpin tip. This information was used to design a *cis*-GP peptide bond mimetic stabilized by a pseudoproline derivative.[60] In another study, a *trans*-GP conformation was stabilized by a spirocyclic Freidinger-like lactam.[61] Several more recent studies have used single or double disulfide-bridges, as well as replacement of P313 by D-Pro, to stabilize and mimic ß-hairpin conformations in V3 loop peptides.[62-64] However, none of these approaches to hairpin mimetic design are as effective as the one reported here in stabilizing the antibody-bound form of the antigen. This is demonstrated here by the very close structural similarity of the mimetic with that of a V3 peptide bound to F425-B4e8 (Figure-4). The use of a D-Pro-L-Pro template to design macrocyclic hairpin mimetics is a straightforward and highly effective approach that should be widely useful in generating accurate structural mimetics of ß-hairpin motifs. We could also show that the mimetic binds to F425-B4e8 with high affinity.

We also tested whether the mimetic displayed on SVLPs (i.e. lipopeptide **4**), is able to elicit F425-B4e8-like antibodies that can bind to gp120, and exhibit HIV-1 neutralising activity. The immunogen (lipopeptide **4**) assembles into nanoparticles in aqueous buffers with a diameter of ca. 20-30 nm, which should display ca. 60-80 copies of the mimetic across the surface of the nanoparticle (Figure-5). The lipopeptide **4** also contains a promiscuous T helper epitope derived from the malaria parasite,[16] and SVLP formation is driven by the presence of a Pam_3Cys moiety, which is a known Toll-Like Receptor (TLR) ligand.[13] These V3 mimetic-coated nanoparticles elicited antibodies in rabbits, without the use of an adjuvant, that indeed bind strongly to recombinant gp120 by ELISA (Figure-6). However, only infection by the neutralization-sensitive laboratory MN strain was successfully inhibited by the anti-mimetic IgG. None of the neutralization-insensitive strains isolated from HIV-infected humans were inhibited, unless the V1V2 loop region was first deleted. All the V1V2

mutant viruses, except REJO were highly sensitive to neutralization by the anti-mimetic antibodies.

The V1V2 variable loop in gp120 exibits length and sequence polymorphism across diverse HIV-1 strains, but its deletion is tolerable and is known to yield replication competent viruses. Moreover, the V1V2 loop has a profound influence on the virus' susceptibility to neutralization, in particular, by shielding neutralizing epitopes in the V3 loop.[65-71] Unmasking of V1V2 reveals potent neutralizing activity by many monoclonal antibodies directed against the V3 loop. The results obtained here with the anti-mimetic antibodies are consistent with this effect, and provide potentially valuable information for future HIV-1 vaccine design. The mechanism of shielding by V1/V2 is of great interest. A recent study concluded that V1V2 protects the V3 loop of a neighboring gp120 in the context of the native trimer in the spikes on the viral surface.[42] Hence, the quaternary structure of gp120 allows inter-subunit contacts that effectively shield cross-neutralization-sensitive epitopes. New strategies are now required to overcome this V1V2 shielding, in order to fully exploit the therapeutic potential of V3 loop cross-reactive antibodies, and V3 loop mimetics in vaccine design.

Experimental Section

Peptide synthesis

All peptides were prepared using Fmoc-chemistry with methods described elsewhere.[14, 16, 33] Full details of synthetic procedures and characterization of products are given in the Supporting Information.

Conformational studies by NMR

^{1}H NMR measurements were performed in H_2O/D_2O (9:1) or pure D_2O, at pH 5.0, at 1-3 mM peptide. Spectra were acquired for structure calculations on a Bruker AV-600 spectrometer at 300 K. Data were processed using TOPSPIN 2.1 (Bruker) or XEASY.[72] Water suppression was performed by presaturation. Spectral assignments were made using 2D DQF-COSY, TOCSY and NOESY spectra. $^3J_{HN\alpha}$ coupling constants were determined from 1D spectra or from 2D NOESY spectra by inverse Fourier transformation of in-phase multiplets.[73]

[^{13}C,^{1}H]-HSQC spectra at natural abundance were recorded in D_2O. Acquisition data were sampled as 1024x512 complex points in t_2 and t_1. The 2D data matrices were multiplied by a square-sine-bell window function and zero-filled to 2x2k points prior to Fourier transformation. Distance restraints were obtained from NOESY spectra with a mixing time of 250 ms. Spectra were typically collected with 1024 x 256 complex data points zero-filled prior to Fourier transformation to 2048 x 1024, and transformed with a cosine-bell weighting function. The structure calculations were performed by restrained molecular dynamics in torsion angle space using DYANA[74] and only NOE-derived distance restraints. Starting from 100 randomized conformations a bundle of 20 final structures were selected, which encur the lowest DYANA target energy function. The program MOLMOL[75] was used for structure analysis and visualization of the molecular models. DYANA structures were optimized by energy minimization using the program MOE (*Chemical Computing Group*, Canada).

Competition ELISA with antibody F425-B4e8

ELISA microtiter plates (*Nunc* Immunoplates Polysorb F96) were coated overnight with streptavidin (5 μg/mL) in carbonate buffer (50 μL, 0.2 M, pH 9.6). The wells were then washed with PBS (10 mM sodium phosphate, 154 mM NaCl, pH 7.2) containing 0.05%

Tween 20 (PBST) and blocked with PBS containing 4% BSA (100 µL) for 1 h. After blocking, the wells were washed three times with PBST and incubated with the peptide biotin-GGGGYNKRKRIHIGPGRAFYTTKNIIG (50 µL, 5 nM) in PBS for 1 h. After washing, antibody F425-B4e8 (40 pM) pre-incubated with a competing ligand in PBS for 2 h, was added for 1 h. After washing with PBST, the plates were incubated with horseradish peroxidase labeled goat anti-human IgG diluted 1:20'000 in PBST containing 0.1 % BSA (50 µL) for 1 h. Color was developed for 30 min using 3,3'-5,5'-tetramethylbenzidine dihydrochloride hydrate (50 µL, 0.3 mg/mL) in Buffer A (100 mM citric acid and 122 mM disodium hydrogen phosphate dihydrate, pH 4.0) containing 0.1 % H_2O_2. After adding a stop solution (50 µL, 2 M H_2SO_4), the absorbance was read at 450 nm using a *SpectraMax* M5 microplate reader. All experiments were conducted in duplicate. Absorbance values were converted into % inhibition using the equation %-inhibition = $(1 - (A/A_o)) \times 100$, where A represents the value in the presence of inhibitor and A_o is the value without inhibitor (see Supporting Information). The IC_{50} was calculated using the program IGOR Pro 6.01 (*WaveMetrix Inc.*).

Determination of anti-mimetic IgG endpoint titres

Microtiter plates (*Nunc* Immunoplates Polysorb F96) were coated overnight with streptavidin (50 µL, 5 µg/mL) in PBS. The wells were then washed with PBS containing 0.05% Tween 20 (PBST) and blocked with PBS containing 4% BSA (100 µL) for 1h. The wells were then washed three times with PBST and incubated with **mimetic (1)** coupled through a PEG linker to biotin (**biotinyl-PEG-mimetic** (**6**)) (for the synthesis of this ligand see Supporting Information) in PBS (50 µL, 1.5 µg/mL). After washing with PBST the plates were incubated with serial dilutions of rabbit sera (50 µL) in PBS containing 0.05% Tween 20 and 0.5 % skim milk powder (MPBST) for 2.5 h, followed by three washes with PBST. The plates were

then incubated with alkaline phosphatase-conjugated mouse anti-rabbit IgG antibody (*Sigma*, γ-chain specific), diluted 1:20'000 in MPBST (50 µL) for 1 h, washed again three times with PBST and incubated in the dark with *p*-nitrophenyl phosphate (*Sigma*) (50 µL, 1 mg/mL) in sodium carbonate buffer (50 mM) containing $MgCl_2$ (1mM, pH 9.6). The absorbance was measured at 405 nm using a *SpectraMax* M5 microplate reader.

Binding of anti-mimetic IgG to gp120

$Gp120_{JRFL}$ (*Progenics*) was diluted with coating buffer (0.05 M sodium carbonate, pH 9.6) to a final concentration of 2.5 µg/mL, and aliquots (50 µL) were used to coat wells of a microtiter plate (Maxisorp, *Nunc*) overnight at 4 ºC. After washing with PBST, wells were blocked with PBS containing 5% skim milk powder (100 µL per well) for 30 min. After washing, polyclonal IgG (50 µL, 10 µg/mL) isolated from rabbit serum was pre-incubated with serial dilutions of the competing peptide mimetic (50µL per well) in PBS for 1 h, and then dispensed into wells and incubated for 1 h. After washing, alkaline phosphatase-conjugated mouse anti-rabbit IgG antibody (*Sigma*, γ-chain specific, diluted 1:20'000 in MPBST, 50 µL) was added to each well and incubated for 1 h. The plate was washed with PBST and then incubated in the dark with *p*-nitrophenyl phosphate (*Sigma*) (50 µL, 1 mg/mL) in sodium carbonate (50 mM) with $MgCl_2$ (1 mM, pH 9.6). The absorbance was measured at 405 nm using a *SpectraMax* M5 microplate reader. All experiments were conducted in duplicates. Error bars indicate standard deviations of duplicate determinations (Figure-6A). The data were analyzed using the program IGOR Pro 6.01 (*WaveMetrix Inc.*).

Neutralization assays

The origins of the HIV-1 strains, the generation of V1V2-deleted envelopes, and the neutralization assays with Env-pseudotyped virus were performed as described earlier.[42]

Acknowledgements

The authors thank the Swiss National Science Foundation for financial support. The following reagent was obtained through the AIDS Research and Reference Reagent Program, Division of AIDS, NIAID, NIH: antibody F425-B4e8 from Dr. Marshall Posner and Dr. Lisa Cavacini.

Keywords

peptide, lipopeptide, vaccine,virus-like particle, conformation, antibody, vaccine

References

[1] S. A. Plotkin, *Clin. Vacc. Immunol.* **2009**, *16*, 1709.

[2] B. Pulendran, R. Ahmed, *Nat. Immunol.* **2011**, *12*, 509.

[3] A. Sette, R. Rappuoli, *Immunity* **2010**, *33*, 530.

[4] R. L. Coffman, A. Sher, R. A. Seder, *Immunity* **2010**, *33*, 492.

[5] M. L. Mbow, E. De Gregorio, N. M. Valiante, R. Rappuoli, *Curr. Opin. Immunol.* **2010**, *22*, 411.

[6] D. Hans, P. R. Young, D. P. Fairlie, *Med. Chem.* **2006**, *2*, 627.

[7] N. E. Harwood, F. D. Batista, *Annu. Rev. Immunol.* **2010**, *28*, 185.

[8] F. D. Batista, N. E. Harwood, *Nat. Revs. Immunol.* **2009**, *9*, 15.

[9] D. R. Fooksman, S. Vardhana, G. Vasiliver-Shamis, J. Liese, D. A. Blair, J. Waite, C. Sacristán, G. D. Victora, A. Zanin-Zhorov, M. L. Dustin, *Annu. Rev. Immunol.* **2010**, *28*, 79.

[10] E. Segura, J. A. Villadangos, *Curr. Opin. Immunol.* **2009**, *21*, 105.

[11] S. F. Gonzalez, S. E. Degn, L. A. Pitcher, M. Woodruff, B. A. Heesters, M. C. Carroll, *Annu. Rev. Immunol.* **2011**, *29*, 215.

[12] T. Kawai, S. Akira, *Nat. Immunol.* **2010**, *11*, 373.

[13] I. Botos, D. M. Segal, D. R. Davies, *Structure* **2011**, *19*, 447.

[14] F. Boato, R. M. Thomas, A. Ghasparian, A. FreundRenard, K. Moehle, J. A. Robinson, *Angew. Chem. Int. Ed.* **2007**, *46*, 9015.

[15] A. W. Perriman, D. S. Williams, A. J. Jackson, I. Grillo, J. M. Koomullil, A. Ghasparian, J. A. Robinson, S. Mann, *Small* **2010**, *6*, 1191.

[16] A. Ghasparian, T. Riedel, J. Koomullil, K. Moehle, C. Gorba, D. I. Svergun, A. W. Perriman, S. Mann, M. Tamborrini , G. Pluschke , J. A. Robinson, *ChemBioChem* **2011**, *12*, 100.

[17] J. Y. Kang, X. Nan, M. S. Jin, S.-J. Youn, Y. H. Ryu, S. Mah, S. H. Han, H. Lee, S.-G. Paik, J.-O. Lee, *Immunity* **2009**, *31*, 873.

[18] M. S. Jin, S. E. Kim, J. Y. Heo, M. E. Lee, H. M. Kim, S.-G. Paik, H. Lee, J.-O. Lee, *Cell* **2007**, *130*, 1071.

[19] S.-R. Wu, R. Löving, B. Lindqvist, H. Hebert, P. J. B. Koeck, M. Sjöberg, H. Garoff, *Proc. Nat. Acad. Sci. USA* **2010**, *107*, 18844.

[20] R. Wyatt, J. Sodroski, *Science* **1998**, *280*, 1884.

[21] C. C. Huang, S. N. Lam, P. Acharya, M. Tang, S. H. Xiang, S. S. Hussan, R. L. Stanfield, J. Robinson, J. Sodroski, I. A. Wilson, R. Wyatt, C. A. Bewley, P. D. Kwong, *Science* **2007**, *317*, 1930.

[22] B. L. Wu, E. Y. T. Chien, C. D. Mol, G. Fenalti, W. Liu, V. Katritch, R. Abagyan, A. Brooun, P. Wells, F. C. Bi, D. J. Hamel, P. Kuhn, T. M. Handel, V. Cherezov, R. C. Stevens, *Science* **2010**, *330*, 1066.

[23] L. E. E. Ratner, A. Fisher, L. L. Jagodzinski, H. Mitsuya, R.-S. Liou, R. C. Gallo, F. Wong-Staal, *AIDS Res. Hum. Retroviruses* **1987**, *3*, 57.

[24] C. C. Huang, M. Tang, M. Y. Zhang, S. Majeed, E. Montabana, R. L. Stanfield, D. S. Dimitrov, B. Korber, J. Sodroski, I. A. Wilson, R. Wyatt, P. D. Kwong, *Science* **2005**, *310*, 1025.

[25] R. L. Stanfield, M. K. Gorny, C. Williams, S. Zolla-Pazner, I. A. Wilson, *Structure* **2004**, *12*, 193.

[26] R. L. Stanfield, M. K. Gorny, S. Zolla-Pazner, I. A. Wilson, *J. Virol.* **2006**, *80*, 6093.

[27] C. H. Bell, R. Pantophlet, A. Schiefner, L. A. Cavacini, R. L. Stanfield, D. R. Burton, I. A. Wilson, *J. Mol. Biol.* **2008**, *375*, 969.

[28] A. K. Dhillon, R. L. Stanfield, M. K. Gorny, C. Williams, S. Zolla-Pazner, I. A. Wilson, *Acta. Crystall. D* **2008**, *D64*, 792.

[29] X. Q. Jiang, V. Burke, M. Totrov, C. Williams, T. Cardozo, M. K. Gorny, S. Zolla-Pazner, X. P. Kong, *Nat. Struct. Mol. Biol.* **2010**, *17*, 955.

[30] C. H. Bell, R. Pantophlet, A. Schiefner, L. A. Cavacini, R. L. Stanfield, D. R. Burton, I. A. Wilson, *J. Mol. Biol.* **2008**, *375*, 969.

[31] R. Pantophlet, R. O. Aguilar-Sino, T. Wrin, L. A. Cavacini, D. R. Burton, *Virology* **2007**, *364*, 441.

[32] J. A. Robinson, *Acc. Chem. Res.* **2008**, *41*, 1278.

[33] L. Jiang, K. Moehle, B. Dhanapal, D. Obrecht, J. A. Robinson, *Helv. Chim. Acta.* **2000**, *83*, 3097.

[34] K. Wüthrich, *NMR of proteins and nucleic acids*, J. Wiley & Sons, New York, **1986**.

[35] N. J. Baxter, M. P. Williamson, *J. Biomol. NMR* **1997**, *9*, 359.

[36] T. Cierpicki, J. Otlewski, *J. Biomol. NMR* **2001**, *21*, 249.

[37] D. S. Wishart, B. D. Sykes, F. M. Richards, *Biochemistry* **1992**, *31*, 1647.

[38] R. M. Fesinmeyer, F. M. Hudson, K. A. Olsen, G. W. N. White, A. Euser, N. H. Andersen, *J. Biomol. NMR* **2005**, *33*, 213.

[39] I. Shu, J. M. Stewart, M. Scian, B. L. Kier, N. H. Andersen, *J. Am. Chem. Soc.* **2011**, *133*, 1196.

[40] D. S. Wishart, *Prog. NMR Spectr.* **2011**, *58*, 62.

[41] P. Rusert, A. Mann, M. Huber, V. von Wyl, H. F. Gunthard, A. Trkola, *AIDS* **2009**, *23*, 1319.

[42] P. Rusert, A. Krarup, C. Magnus, O. F. Brandenberg, J. Weber, A. K. Ehlert, R. R. Regoes, H. F. Gunthard, A. Trkola, *J. Exp. Med.* **2011**, *208*, 1419.

[43] A. Nuccitelli, R. Cozzi, L. J. Gourlay, D. Donnarumma, F. Necchi, N. Norais, J. L. Telford, R. Rappuoli, M. Bolognesi, D. Maione, G. Grandi, C. D. Rinaudo, *Proc. Natl. Acad. Sci. U S A* **2011**, *108*, 10278.

[44] J. M. Rini, R. L. Stanfield, E. A. Stura, P. A. Salinas, A. T. Profy, I. A. Wilson, *Proc. Natl. Acad. Sci. USA* **1993**, *90*, 6325.

[45] J. B. Ghiara, E. A. Stura, R. L. Stanfield, A. T. Profy, I. A. Wilson, *Science* **1994**, *264*, 82.

[46] R. Stanfield, E. Cabezas, A. Satterthwait, E. Stura, A. Profy, I. Wilson, *Structure Fold. Des.* **1999**, *7*, 131.

[47] R. L. Stanfield, J. B. Ghiara, E. Ollmann Saphire, A. T. Profy, I. A. Wilson, *Virology* **2003**, *315*, 159.

[48] K. Chandrasekhar, A. T. Profy, H. J. Dyson, *Biochemistry* **1991**, *30*, 9187.

[49] P. Catasti, J. D. Fontenot, E. M. Bradbury, G. Gupta, *J. Biol. Chem.* **1995**, *270*, 2224.

[50] W. F. Vranken, F. Fant, M. Budinsky, F. A. M. Borremans, *Eur. J. Biochem.* **2001**, *268*, 2620.

[51] J. B. Ghiara, D. C. Ferguson, A. C. Satterthwait, H. J. Dyson, I. A. Wilson, *J. Mol. Biol.* **1997**, *266*, 31.

[52] E. Cabezas, A. C. Satterthwait, *J. Am. Chem. Soc.* **1999**, *121*, 3862.

[53] E. Cabezas, M. Wang, P. W. Parren, R. L. Stanfield, A. C. Satterthwait, *Biochemistry* **2000**, *39*, 14377.

[54] R. L. Tolman, M. A. Bednarek, B. A. Johnson, W. J. Leanza, S. Marburg, D. J. Underwood, E. A. Emini, A. J. Conley, *Int. J. Pept. Prot. Res.* **1993**, *41*, 455.

[55] A. J. Conley, P. Conard, S. Bondy, C. A. Dolan, J. Hannah, W. J. Leanza, S. Marburg, M. Rivetna, V. K. Rusiecki, E. E. Sugg, F. Van Middlesworth, S. A. Warne, J. Terry Ulrich, J. A. Rudbach, R. L. Tolman, E. A. Emini, *Vaccine* **1994**, *12*, 445.

[56] V. Tugarinov, A. Zvi, R. Levy, J. Anglister, *Nat. Struct. Biol.* **1999**, *6*, 331.

[57] V. Tugarinov, A. Zvi, R. Levy, Y. Hayek, S. Matsushita, J. Anglister, *Struct. Fold Des.* **2000**, *8*, 385.

[58] O. Rosen, J. Chill, M. Sharon, N. Kessler, B. Mester, S. Zolla-Pazner, J. Anglister, *Biochemistry* **2005**, *44*, 7250.

[59] O. Rosen, M. Sharon, S. R. Quadt-Akabayov, J. Anglister, *Proc. Natl. Acad. Sci. USA* **2006**, *103*, 13950.

[60] A. Wittelsberger, M. Keller, L. Scarpellino, L. Patiny, H. Acha-Orbea, M. Mutter, *Angew. Chem. Int. Ed.* **2000**, *39*, 1111.

[61] R. D. Long, K. D. Moeller, *J. Am. Chem. Soc.* **1997**, *119*, 12394.

[62] B. Mester, R. Manor, A. Mor, B. Arshava, O. Rosen, F. X. Ding, F. Naider, J. Anglister, *Biochemistry* **2009**, *48*, 7867.

[63] A. Mor, E. Segal, B. Mester, B. Arshava, O. Rosen, F. X. Ding, J. Russo, A. Dafni, F. Schvartzman, T. Scherf, F. Naider, J. Anglister, *Biochemistry* **2009**.

[64] A. Moseri, S. Tantry, Y. Sagi, B. Arshava, F. Naider, J. Anglister, *Virology* **2010**, *401*, 293.

[65] I. Bontjer, A. Land, D. Eggink, E. Verkade, K. Tuin, C. Baldwin, G. Pollakis, W. A. Paxton, I. Braakman, B. Berkhout, R. W. Sanders, *J. Virol.* **2009**, *83*, 368.

[66] J. Cao, N. Sullivan, E. Desjardin, C. Parolin, J. Robinson, R. Wyatt, J. Sodroski, *J. Virol.* **1997**, *71*, 9808.

[67] C. J. Saunders, R. A. McCaffrey, I. Zharkikh, Z. Kraft, S. E. Malenbaum, B. Burke, C. Cheng-Mayer, L. Stamatatos, *J. Virol.* **2005**, *79*, 9069.

[68] L. Stamatatos, C. Cheng-Mayer, *J. Virol.* **1998**, *72*, 7840.

[69] L. Stamatatos, M. Wiskerchen, C. Cheng-Mayer, *AIDS Res. Hum. Retroviruses* **1998**, *14*, 1129.

[70] R. Wyatt, J. Moore, M. Accola, E. Desjardin, J. Robinson, J. Sodroski, *J. Virol.* **1995**, *69*, 5723.

[71] R. Wyatt, N. Sullivan, M. Thali, H. Repke, D. Ho, J. Robinson, M. Posner, J. Sodroski, *J. Virol.* **1993**, *67*, 4557.

[72] C. Bartels, T.-h. Xia, M. Billeter, P. Güntert, K. Wüthrich, *J. Biomol. NMR* **1995**, *6*, 1.

[73] T. Szyperski, P. Güntert, G. Otting, K. Wüthrich, *J. Mag. Res.* **1992**, *99*, 552.

[74] P. Guntert, C. Mumenthaler, K. Wuthrich, *J. Mol. Biol.* **1997**, *273*, 283.

[75] R. Koradi, M. Billeter, K. Wuthrich, *J. Mol. Graph.* **1996**, *14*, 51.

Table-1. Experimental distance restraints and statistics for the final 20 NMR structures (shown in Figure-4) calculated for the mimetic using DYANA.[74]

	results
NOE upper-distance limits: total Intraresidue Sequential Medium-and longe range	144 42 62 40
Residual target function value ($Å^2$)	0.96 ± 0.05
Mean rmsd value (Å) All backbone atoms All heavy atoms	 1.01 ± 0.50 2.03 ± 0.63
Residual NOE violations Number > 0.2 Å Maximum (Å)	 5 0.28

Figures

Figure-1. **A**, Crystal structures of engineered HIV-1 gp120 core (pink) (with V1V2 loop deleted) with an intact V3 (red), bound to CD4 (green) and an antibody Fab fragment (blue). *Left*, structure PDB 2B4C; *right*, structure PDB 2QA. **B**, V3 loop sequences from the viral strains shown with the location of base, stem and tip (crown) regions. The flanking Cys residues are linked by a disulfide bond in gp120.

A

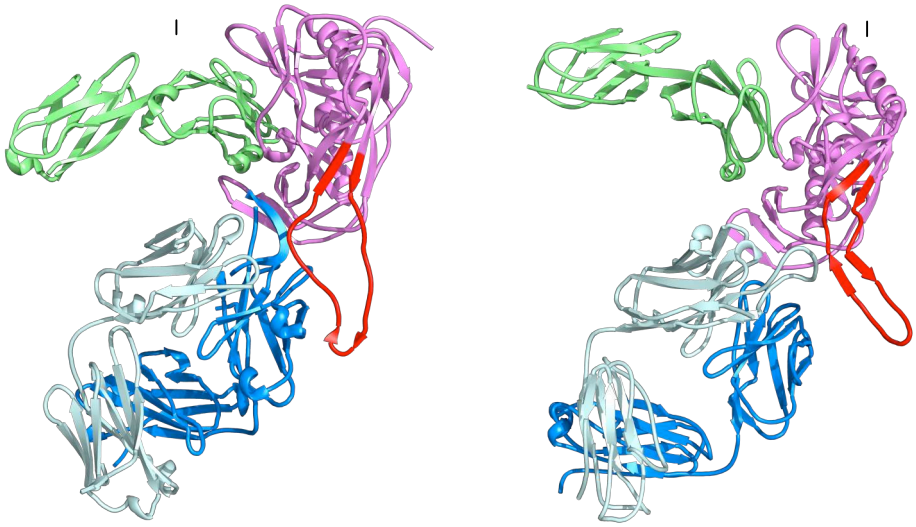

B

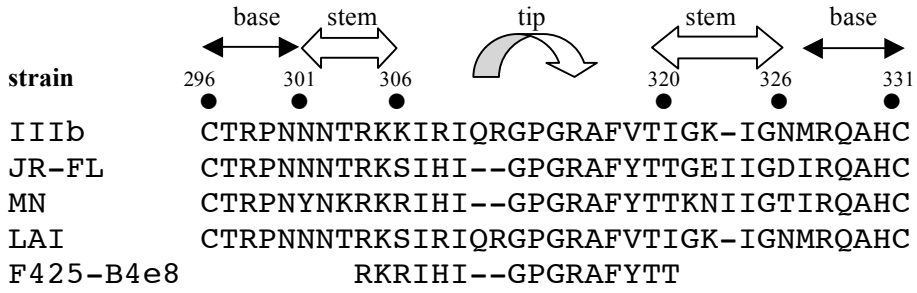

Figure-2. **A**, Ribbon representation of the crystal structure PDB 2QSC showing the V3 peptide (green) bound to the antibody F425-B4e8. **B**, The antibody-bound V3 loop conformation with cross-strand hydrogen bonding (HB) shown by dotted lines, and selected ß-carbons shown as balls. The hairpin mimetic (*right*) is shown with dotted boxes to indicate cross-strand HB pairs.

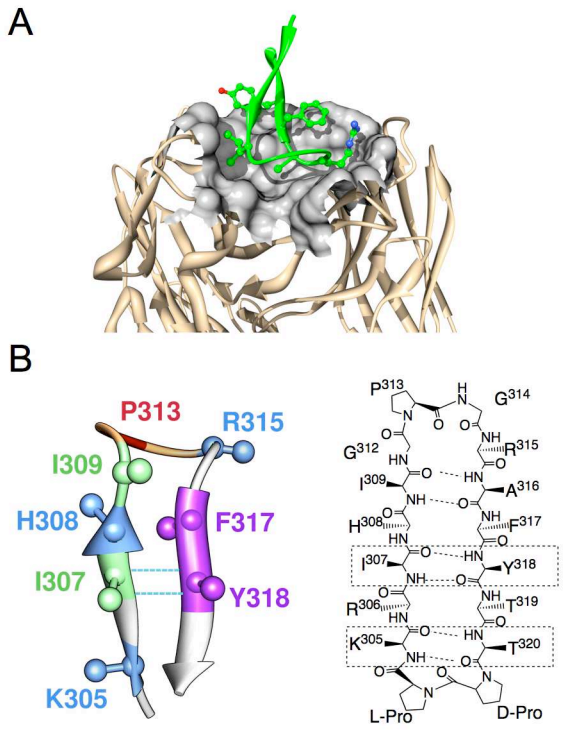

Figure-3. *Top*, $^{3}J_{HNH\alpha}$ (Hz) and -Δδ/T (ppb/K) values for the mimetic. *Bottom*, key cross-strand NOE connectivities observed in ^{1}H NMR 2D-NOESY plots for the mimetic. The observed NOEs are indicated by dotted arrows.

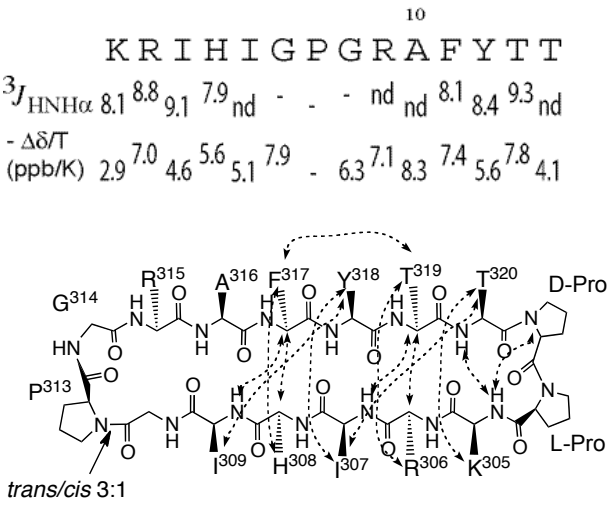

Figure-4. *Top*, Average solution NMR structures for the mimetic; (*left*) all structures backbone-superimposed; (*middle*) one typical structure (Ile, green; Phe, dark pink; Tyr, light pink; Pro, orange; Gly, yellow); (*right*) comparisons of NMR (blue) with the corresponding antibody-bound V3 loop structure (orange) (see text). *Bottom*, Superimposition of the NMR structure of mimetic (*red*) with the linear peptide (*purple*) bound to F425-B4e8 in crystal structure PDB 2QSC.

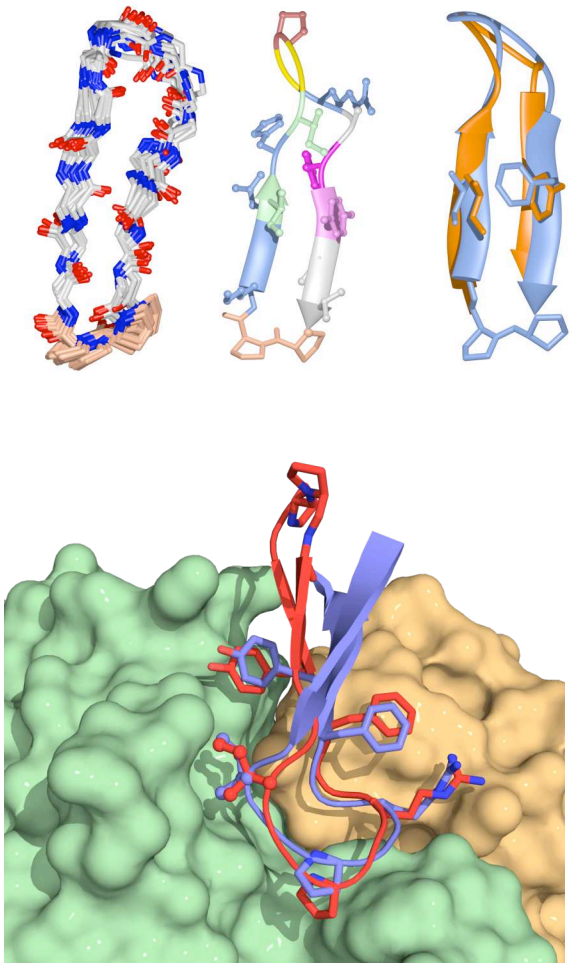

Figure-5. **A**, A hydrazino-derivative of mimetic **1** was coupled to lipopeptide **3**, to give **4**, which spontaneously assembles into 20-25 nm nanoparticles (SVLPs) in buffered solution. **B**, A computer model of the nanoparticle, with 72 copies of the loop mimetic (**1**) shown in red on the surface, and the coiled coil in blue/yellow. The lipid chains are buried in the core of the particle.[15, 16]

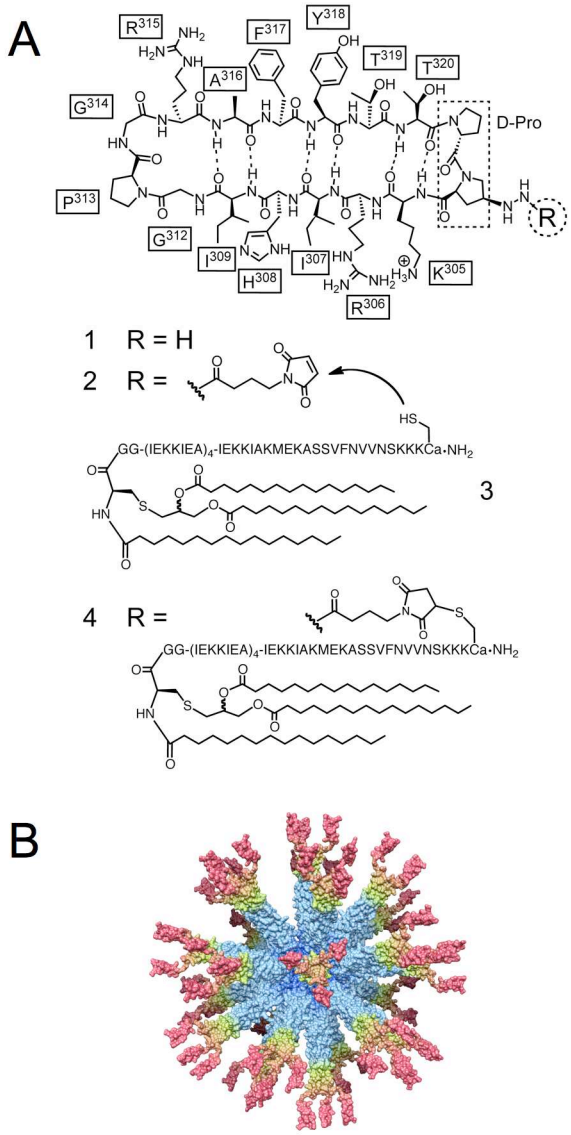

Figure-6. Immunogenicity of lipopeptide-mimetic (**4**). **A**, Inhibition of anti-**4** IgG binding to immobilized gp120 by ELISA; binding is inhibited by increasing concentrations (in μM) of mimetic. **B**, Neutralizing activity of rabbit anti-**4** IgG against molecularly cloned Env-pseudotyped HIV-1 viruses, including wild-type (WT) envelope of strains MN, 10.14, SF162, JR-FL and REJO, and mutant envelopes with the V1V2 loop deleted (see text). **C**, Neutralizing activity of rabbit anti-**4** IgG (tested at 25 and 50 μg/ml, from 2° immunization, rabbit A) was probed at the indicated concentrations for inhibitory activity against MN and 10.14-ΔV1V2 in the presence and absence of competing mimetic (10 μM); showing that the neutralizing activity can be competed-out by free mimetic.

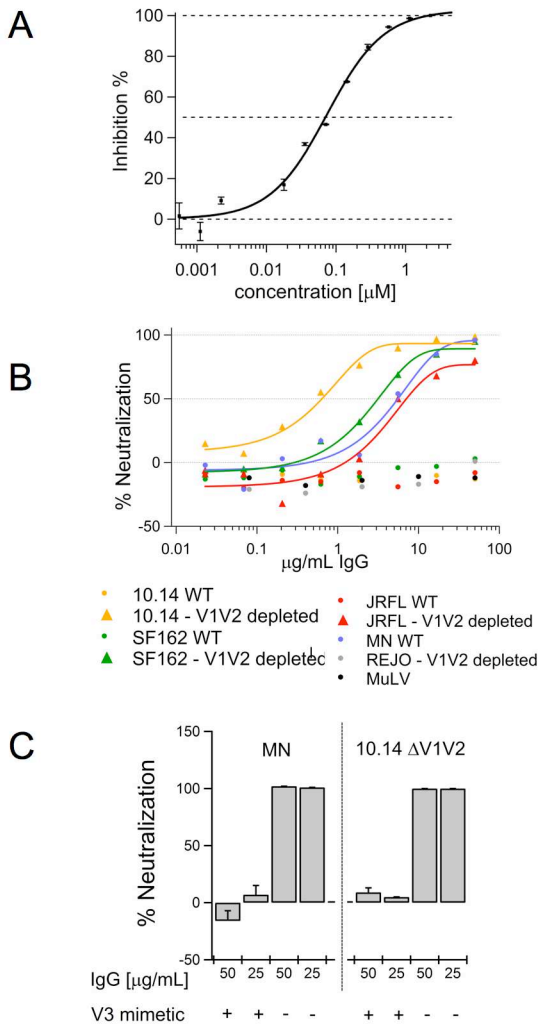

Graphic for Table of Contents

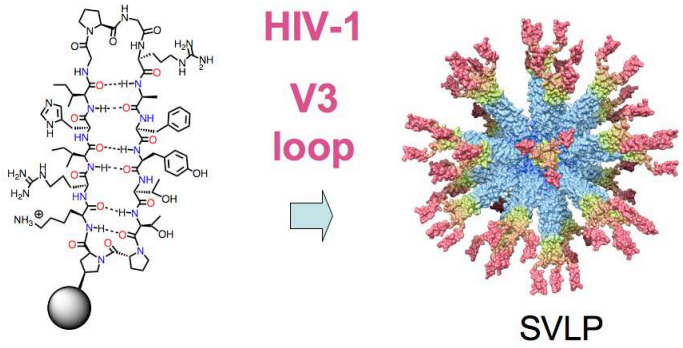

A structural vaccinology approach may lead to a new generation of vaccine candidates, based upon conformationally constrained epitope mimetics. Here a ß-hairpin mimetic of the HIV-1 V3 loop is rendered immunogenic by multivalent display on the surface of synthetic virus-like particles (SVLPs).

Supporting Information

ß-Hairpin Peptidomimetics of the Immunogenic V3 Loop of HIV-1 glycoprotein gp120

Tina Riedel[1], Arin Ghasparian[1], Kerstin Moehle[1], Peter Rusert[2], Alexandra Trkola[2] and John A. Robinson[1]*

[1] Chemistry Department, and [2] Institute of Medical Virology,
University of Zurich, Winterthurerstrasse 190, 8057 Zurich, Switzerland.

1. Abbreviations

Boc, t-butoxycarbonyl; DIEA, *N*,*N*-diiso-propylethylamine, DCM, dichloromethane, DMF, *N,N*-dimethylformamide; Fmoc, 9-fluorenylmethoxycarbonyl; HATU, 2-(1H-7-azabenzotriazol-1-yl)-1,1,3,3-tetramethyluronium hexafluorophosphate; HBTU, 2-[1H-benzotriazole-1-yl]-1,1,3,3-tetramethyluronium hexafluoro-phosphate; HOAt, 1-hydroxy-7-azabenzotriazole; HOBt, 1-hydroxybenzotriazole; Pbf, 2,2,4,6,7-pentamethyldihydrobenzofuran-5-sulfonyl; PyBOP, benzotriazole-1-yloxy-tris-pyrrolidino-phosphonium hexafluorophosphate ; TIS, triisopropylsilane; TFA, trifluoroacetic acid; Trt, trityl.

2. Synthesis of the V3 hairpin mimetic

Peptide synthesis was initiated with Fmoc-D-Pro-OH pre-loaded on 2-chlorotrityl chloride resin on a 0.25 mmol scale. The protected amino acids used were Fmoc-Ala-OH, Fmoc-Arg(Pbf)-OH, Fmoc-Gly-OH, Fmoc-His(Trt)-OH, Fmoc-Ile-OH, Fmoc-Lys(Boc)-OH, Fmoc-Pro-OH, Fmoc-D-Pro-OH, Fmoc-Phe-OH, Fmoc-Thr(*t*Bu)-OH, Fmoc-Tyr(*t*Bu)-OH. The synthetic method was described earlier.[1]

Peptides were purified by preparative RP-HPLC (*Waters* C18 XBridge 5 µm, 300 Å, 19 x 50 mm) using a linear gradient of 10-40% MeCN in water with 0.1% TFA in 20 min at 14 mL/min. HPLC fractions containing the desired product were pooled, frozen and lyophilized. Peptides were analyzed by MALDI-TOF MS and analytical RP-HPLC (*Dr. Maisch* ReproSil Gold C18, 5 µm, 4 x 250 mm or *Agilent* Zorbax Eclipse XDB-C18, 5 µm, 4.6 x 250 mm) using a gradient of 10-60% MeCN in water with 0.1% TFA in 12 min at 0.7 mL/min. t_R = 6.99 min. MALDI-MS *m/z* 1793.0 (calc. 1793.0).

3. Synthesis of hydrazino-mimetic (1)

The peptide Gly-Ile-His(Trt)-Ile-Arg(Pbf)-Lys(Boc) was assembled (0.2 mmol scale) using standard Fmoc chemistry on 2-chlorotrityl resin (*Novabiochem*, loading 0.7 mmol g^{-1}) and HBTU/HOBt/DIPEA for activation. (2*S*,4*R*)-*N*-Benzyloxycarbonyl-4-(*N',N'N'*-tri-tert-butoxycarbonyl-hydrazino)proline (0.28 mmol, 0.19 g, 1.4 eq) was coupled manually to the resin bound peptide chain using HATU (0.3 mmol, 0.114 g, 1.5 eq) in DMF (5 mL) and DIEA (0.6 mmol, 100 µL, 2 eq), with shaking for 75 min at room temp, then the solution was filtered and the resin was washed with DMF (3x 5 mL) and DCM (3x 5 mL). Assembly of the peptide chain was then completed using standard Fmoc chemistry. The resin-bound peptide was treated seven times with a solution of 20 % piperidine in DMF (v/v) (5 mL). The resin was washed with DMF (5 x 5 mL) and DCM (4 x 5 mL) and dried over KOH pellets *in*

vacuo. The linear peptide was cleaved from the resin using 0.6 % TFA in DCM (10 x 5 mL, each 30 s). The filtrate was collected in a flask containing a solution of DIEA (200 µL) in DCM (5 mL). The solvent was evaporated *in vacuo*. The residue dissolved in DMF (30 mL) was treated with HOBt (0.31 mmol, 47.3 mg, 3 eq), PyBOP (0.30 mmol, 154.6 mg, 3 eq) and DIEA (0.87 mmol, 144 µL, 9 eq) was added under argon. After stirring overnight at room temp, DMF was removed *in vacuo*. The peptide was precipitated with cold water (50 mL) and collected by filtration. A solution of TFA:TIS:H_2O (95 : 2.5 : 2.5 (v:v:v); 10 mL) was added. After stirring for 1.5 h at room temp, TFA was removed by evaporation *in vacuo* and the peptide was precipitated with ice-cold Et_2O, washed with ice-cold $Et_2O$and then air-dried. The peptide was purified by preparative RP-HPLC on a C18 column (*Waters XBridge C18, 50x19 mm, 5 µm, 135 Å*) using a gradient of 5 to 60 % MeCN in water (+ 0.05% formic acid) over 10 min at 14 mL/min (t_R=3.62 min) to give a white powder. Yield: 8.8 mg. The peptide (>95%) was characterized by analytical RP-HPLC (*Agilent* Zorbax Eclipse XDB-C18, 5 µm, 4.6 x 250 mm; gradient: 10 to 60 % MeCN in H_2O containing 0.1 % TFA at 1 mL/min); t_R = 9.63; ESI-MS *m/z* 1822.8 $[M+H]^+$; 912.1 $[M+2H]^{2+}$; 608.0 $[M+3H]^{3+}$, MALDI-TOF 1822.9 $[M+H]^+$; *m/z* calculated for $C_{84}H_{132}N_{27}O_{19}$ 1823.0 $[M+H]^+$.

4. Synthesis of peptide 2

A solution of *N*-succinimidyl-4-maleimidobutyrate (*Sigma*) (1.0 mg, 3.6 µmol, 1.0 eq) in H_2O/THF (1:1, 150 µL) was added to a solution of **peptide 1** (6.6 mg, 3.6 µmol) in H_2O (3 mL) and the pH was adjusted to 5.3 by adding 0.1 M NaOH. The reaction mixture was stirred for 1 h at room temp. The product was purified by semipreparative RP-HPLC (*Interchim*, Interchrom C4, 250 x 10 mm, 5 µm, 300 Å) using a gradient of 25 to 60% MeCN in H_2O (+ 0.1% TFA) over 7 min. t_R = 5.58 min (yield: 3.9 mg, 55 %). Analytical RP-HPLC (*Interchim*, Interchrom *UP5WC4-25QS*, 10 to 100% MeCN in H_2O (+ 0.1% TFA) over 17

min at 1 mL/min: purity > 98%. t_R = 9.16 min. ESI-MS *m/z* 497.9 $[M+4H]^{4+}$; 663.3 $[M+3H]^{3+}$; 994.8 $[M+2H]^{2+}$; *m/z* calculated for $C_{92}H_{138}N_{28}O_{22}$ 1988.1 $[M+H]^{+}$.

5. Synthesis of lipopeptide 4

A solution of **lipopeptide 3** (prepared as described earlier [2]) (0.54 μmol, 3.8 mg) in H_2O / MeCN (1:1, 1 mL) was added to a stirred solution of peptide **peptide 2** (0.70 μmol, 1.4 mg, 1.3 eq) in H_2O/MeCN (1:1, 0.5 mL) and the pH was adjusted to 6.5 by adding 0.1 M NaOH. After stirring for 1.5 h at room temp, the solution was lyophilized and the crude product was dissolved in H_2O/MeCN (1:1, 2 mL) containing 0.1 % TFA and purified by semipreparative RP-HPLC on a C4 column (*Interchrom*) using a gradient of 30 to 100 % MeCN in water (+0.1% TFA) over 21 min followed by a wash with 100 % MeCN over 4 min at 4.5 mL/min (t_R = 23.21 min). Yield: 3.0 mg. Purity was > 95 % by analytical RP-HPLC on a C4 column (*Interchrom*) using a gradient of 30 to 100 % MeCN in water (+0.1% TFA) over 14 min at 1 mL/min followed by a wash with 100 % MeCN over 4 min at 1 mL/min (t_R = 17.57 min). ESI-MS (positive mode) *m/z* 1504.9 $[M+6H]^{6+}$; 1290.2 $[M+7H]^{7+}$; 1128.9 $[M+8H]^{8+}$; 1003.7 $[M+9H]^{9+}$; 903.0 $[M+10H]^{10+}$; 820.9 $[M+11H]^{11+}$, 752.6 $[M+12H]^{12+}$, 694.8 $[M+13H]^{13+}$; *m/z* 9021.6 ± 0.03%; MALDI-TOF 9023.7 $[M+H]^{+}$; *m/z* calculated for $C_{420}H_{721}N_{102}O_{108}S_3$ 9023.2 $[M+H]^{+}$.

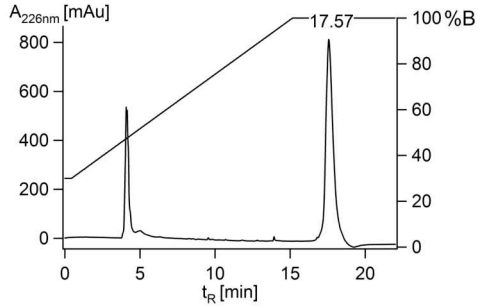

Analytical RP-HPLC chromatogram of **peptide 4** (*Interchim* Interchrom UP5WC4-25QS (C4, 250 x 4.6 mm, 5 μm, 300 Å), gradient: 30 to 100 % MeCN in water (+0.1% TFA) over 14 min at 1 mL/min followed by a wash with 100 % MeCN over 4 min at 1 mL/min (t_R = 17.57 min).

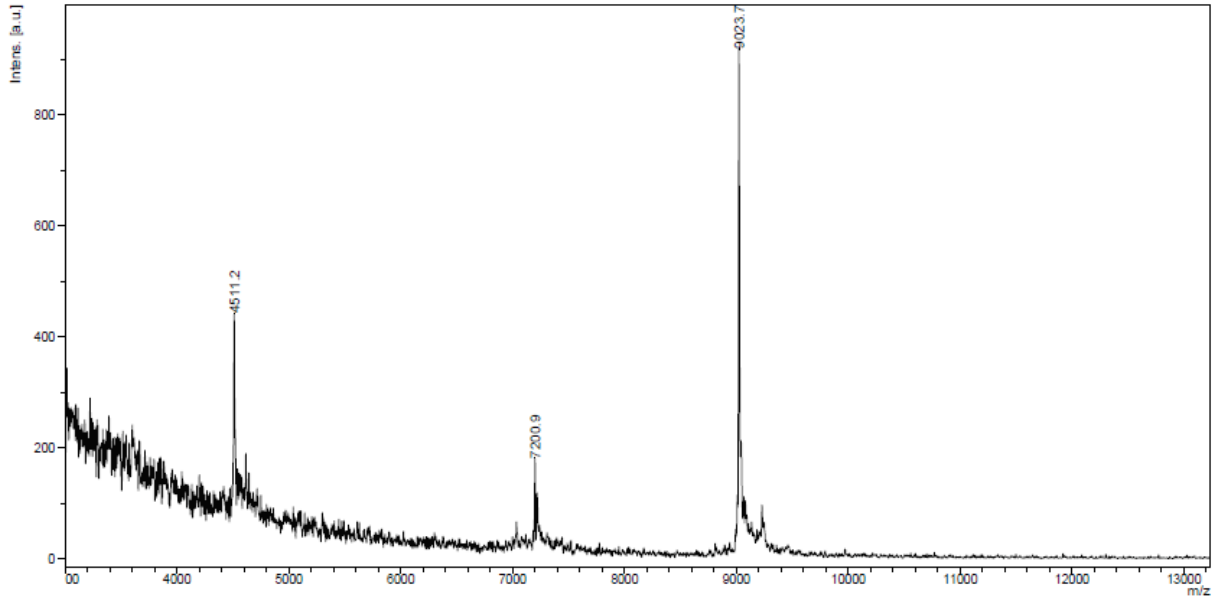

MALDI-MS of **lipopeptide 4**.

When dissolved in PBS, lipopeptide 4 spontaneously forms nanoparticles, as detected by dynamic light scattering (DLS) and electron microscopy (see also ref.[2]). Representative mass-weighted size-distribution of **lipopeptide 4** measured by DLS at a concentration of 1 mg/mL in PBS is shown below. A mean hydrodynamic radius ($R_{h)}$ of 14.8 nm was estimated for all species that contribute > 99 % to the total mass-weighted light-scattering intensity, whereas the main species formed particles with a mean R_h of 13.1 nm.

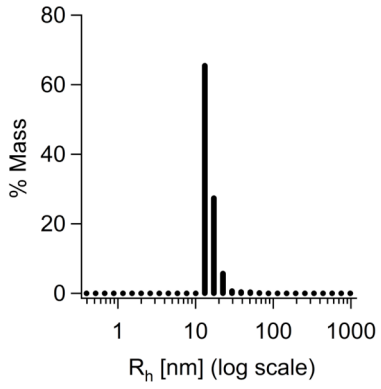

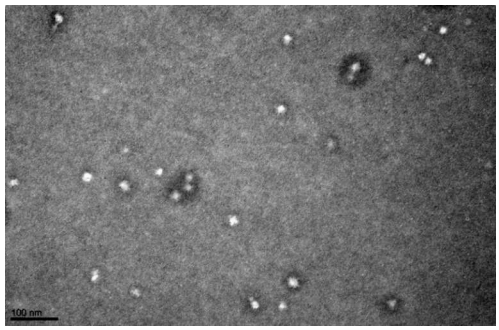

Also shown is a representative electron micrograph of SVLPs formed by **lipopeptide 4** (1 µM) measured in TBS buffer containing 90 mM NaCl at a magnification of 135000x. The

scale bar indicates 100 nm. Particles with a diameter of ~20-25 nm are observed, although some particle aggregates are also seen.

6. Synthesis of biotinyl-PEG-mimetic (6)

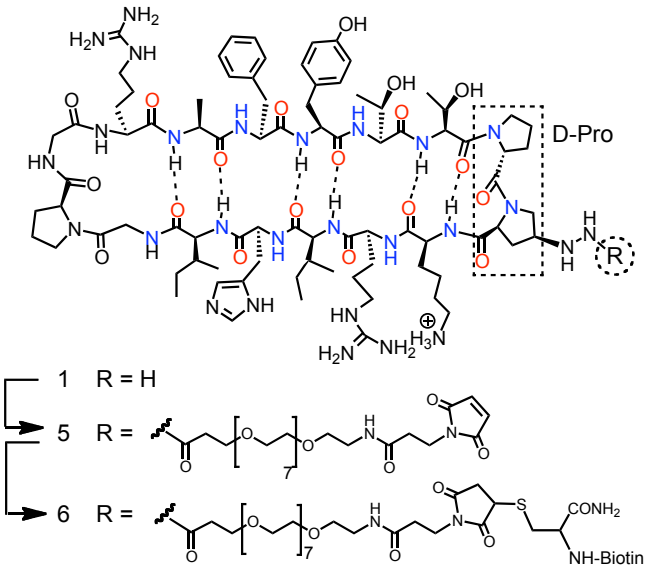

To **peptide 1** (3.2 mg, 1.8 µmol) in H_2O (1 mL) (pH = 5.3) at 0°C was added a solution of *MAL-PEO8-NHS* (*Interchim*) (1.5 mg, 2.1 µmol, 1.2 eq) in THF (500 µL). After stirring for 4 h at room temp. the solution was lyophilized. The product (**5**) was dissolved in 10% MeCN in H_2O + 0.1 % TFA (5 mL) and purified by semipreparative HPLC (Zorbax Eclipse C18) using a gradient from 10 to 100 % MeCN in H_2O + 0.1 % TFA in 14.5 min at 5 mL/min (t_R = 6.04 min). Yield: 2.9 mg. Analytical RP-HPLC (*Agilent* Zorbax Eclipse XDB-C18, 5 µm, 4.6 x 250 mm; gradient: 10 to 100 % MeCN in H_2O containing 0.1 % TFA in 17 min at 1 mL/min) t_R = 7.87; ESI-MS *m/z* 800.0 $[M+3H]^{3+}$; 600.0 $[M+4H]^{4+}$; *m/z* 2396.5±0.02%; *m/z* calculated for $C_{110}H_{174}N_{29}O_{31}$ 2397.3 $[M+H]^{+}$.

A solution of biotinyl-Cys-NH_2 (0.32 mg) and the peptide **5** (1.6 mg) in MeCN/H_2O was stirred for 1 h at pH 6 for coupling to occur. The product (**6**) was purified by analytical RP-HPLC (*Agilent* Zorbax Eclipse XDB-C18, 5 µm, 4.6 x 250 mm; gradient: 10 to 100 % MeCN in H_2O containing 0.1 % TFA in 12 min at 1 mL/min; t_R = 6.79). Yield: 1.8 mg. The

product was obtained in > 98 % purity as assessed by analytical HPLC analysis. ESI-MS *m/z* 915.9 $[M+3H]^{3+}$; 696.9 $[M+4H]^{4+}$; MALDI-TOF *m/z* 2743.3 $[M+H]^{+}$; *m/z* calculated for $C_{123}H_{196}N_{33}O_{34}S_2$ 2743.4 $[M+H]^{+}$.

7. Competition ELISA with antibody F425-B4e8

The results shown below were used to determine IC_{50} values for the hairpin mimetic (solid line) and linear peptide (RP142) (dotted line):

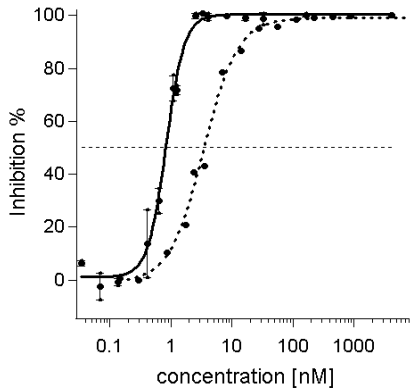

8. Immunization protocol

Immunizations were performed with three New Zealand white rabbits. The lipopeptide **4** was dissolved in PBS and injected intramuscularly (no adjuvant was used) (150 µg of **4** in 400 µl PBS per immunization). Three immunizations were performed on days 1, 28 and 56, and serum was collected on days 0 (pre-immune serum), 14, 38 and 66.

9. IgG Isolation from rabbit serum

Rabbit serum was diluted 1:10 in equilibration buffer (50 mM Tris-HCl, 150 mM NaCl, pH 8.6) and filtered through 0.2 µm filter units (*Whatman*). The diluted serum was loaded onto a pre-equilibrated HiTrap™ Protein G affinity column (*GE Healthcare*) with a flow rate of 0.7 mL/min. After washing away unbound proteins, the bound IgG fraction was eluted with

elution buffer (50 mM glycine-HCl, pH 3.0) at a flow rate of 0.7 mL/min, and neutralized with neutralization buffer (500 mM sodium phosphate, pH 7.6). Neutralization was performed by collecting the IgG fractions into tubes containing 1/5 volume of neutralization buffer. Desalting of the antibody solution into PBS buffer was performed using a HiTrap^{TM} desalting column (5 mL, *GE Healthcare*) at a flow rate of 5 mL/min. The antibody solution was then concentrated to a final concentration of 1-2 mg/mL using a centrifugal filter device (YM-50 Centricon, *Millipore*) and sterile filtered through 0.1 μm filter devices (*Millipore*). The concentration was determined based on the theoretical extinction coefficient of $\varepsilon = 0.203\ M^{-1}cm^{-1}$ (OD = 1.35 for a 1 mg/mL IgG solution). The purity of polyclonal IgG fraction was confirmed by SDS-PAGE, showing bands of 25 kDa for light chains and 50 kDa for heavy chains detected under reducing conditions (4 x SDS buffer containing 12 % SDS, 30 % glycerol, 20 % mercaptoethanol, 4 mM EDTA, 80 mM Tris).

10. Binding of anti-mimetic antibodies to gp120 by SPR (BIAcore)

Recombinant gp120 from strain JR-FL was immobilized on a CM5 sensor chip (*BIAcore*, *GE Healthcare*) by random amine coupling. The isolated IgG fraction from rabbit serum, following the third immunization, was eluted over the sensor using a BIAcore 3000 instrument. The resulting sensorgrams are shown below.

The BIAcore sensograms show the response upon direct binding of polyclonal IgG to immobilized $gp120_{JRFL}$ on the CM5 chip surface. Polyclonal antibody concentrations from top to bottom are 2000 nM, 1000 nM, 500 nM, 250 nM, and 125 nM. The blank lines indicate the fit of recorded data to a 1:1 Langmuir binding model using the BIAevaluation software v.4.0.1. Note that this data cannot be used to determine binding constants, since the antibodies are bivalent and polyclonal. The results demonstrate the presence of antibodies in serum that are able to recognize and bind $gp120_{JRFL}$. As a control, the experiment was

repeated using gp120 from HIV-1 strain LAI, but this gave no BIAcore response (data not shown), indicating that the antibodies are not able to recognize the gp120 from this strain.

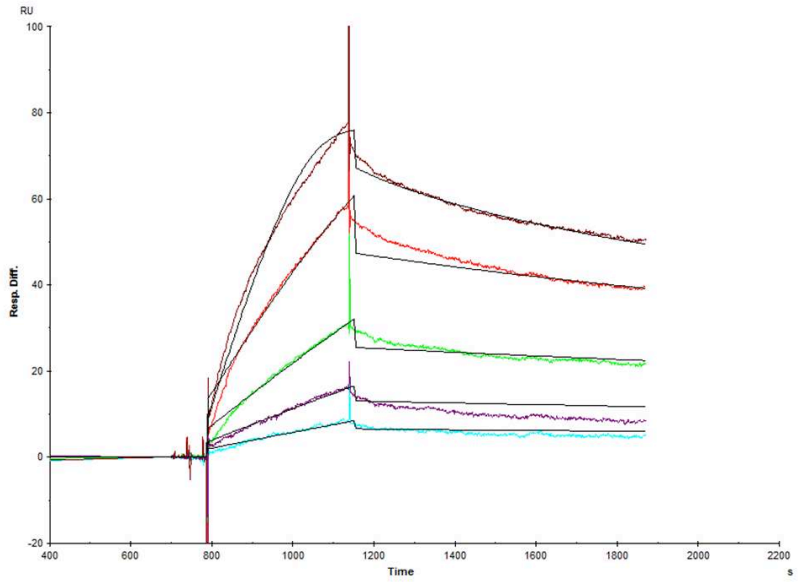

11. NMR Chemical shift deviations from random coil values

Chemical shift deviations from random coil values ($\delta^{observed}$ - δ^{random}) for Hα, Cα and Cß resonances for the mimetic were measured. The results are shown below. For strands in ß-hairpins positive values for $\Delta\delta_{H\alpha}$ and $\Delta\delta_{C\beta}$ and negative values for $\Delta\delta_{C\alpha}$ are expected.[3-6]

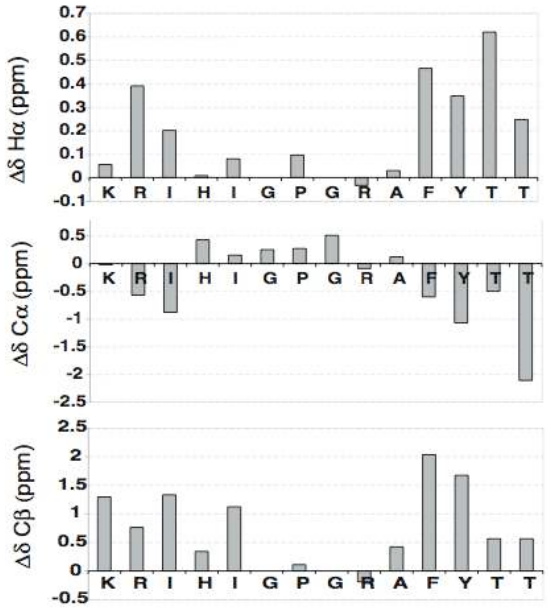

References

1. Jiang, L.; Moehle, K.; Dhanapal, B.; Obrecht, D.; Robinson, J. A., *Helv. Chim. Acta*. **2000**, *83*, 3097-3112.
2. Ghasparian, A.; Riedel, T.; Koomullil, J.; Moehle, K.; Gorba, C.; Svergun, D. I.; Perriman, A. W.; Mann, S.; Tamborrini , M.; Pluschke , G.; Robinson, J. A., *ChemBioChem* **2011**, *12*, 100-109.
3. Wishart, D. S.; Sykes, B. D.; Richards, F. M., *Biochemistry* **1992**, *31*, 1647-1651.
4. Fesinmeyer, R. M.; Hudson, F. M.; Olsen, K. A.; White, G. W. N.; Euser, A.; Andersen, N. H., *J. Biomol. NMR* **2005**, *33*, 213-231.
5. Shu, I.; Stewart, J. M.; Scian, M.; Kier, B. L.; Andersen, N. H., *J. Am. Chem. Soc.* **2011**, *133*, 1196-1199.
6. Wishart, D. S., *Prog. NMR Spectr*. **2011**, *58*, 62-87.